Mon. Not. R. Astron. Soc. **359,** 531–544 (2005) doi:10.1111/j.1365-2966.2005.08917.x

CH stars at high Galactic latitudes

Aruna Goswami★
Indian Institute of Astrophysics, Koramangala, Bangalore 560034, India

Accepted 2005 February 9. Received 2005 February 3; in original form 2004 November 24

ABSTRACT

Carbon-rich stars of Population II, such as CH stars, can provide direct information on the role of low- to intermediate-mass stars of the halo in early Galactic evolution. Thus accurate knowledge of the CH stellar population is a critical requirement for building up scenarios for early Galactic chemical evolution. In the present work, we report on several CH stars identified in a sample of faint high-latitude carbon stars from the Hamburg survey and discuss their medium-resolution spectra covering the wavelength range 4000–6800 Å. Estimation of the depths of the $(1,0)^{12}C^{12}C$ λ4737 and $(1,0)^{12}C^{13}C$ λ4744 bands in these stars indicates an isotopic ratio $^{12}C/^{13}C \sim 3$, apart from a few exceptions; these ratios are consistent with existing theories of CH stellar evolution. The stars of the Hamburg survey, a total of 403 objects, were reported to be carbon star candidates with strong C_2 and CN molecular bands. In the first phase of observation, we acquired spectra of 91 objects. Inspection of the spectra of those objects shows 51 objects with C_2 molecular bands in their spectra, of which 13 stars have low flux below about 4300 Å. There are 25 objects that show weak or moderate CH and CN bands, 12 objects that show weak but detectable CH bands, and three objects that do not show any molecular bands due to C_2, CN or CH in their spectra. Objects with C_2 molecular bands and with good signals bluewards of 4300 Å that show prominent CH bands in their spectra are potential candidate CH stars. There were 35 such candidates found in the present sample of 91 objects observed so far. The set of CH stars identified could be the targets of subsequent observation at high resolution for a detailed and comprehensive analysis to understand their role in early Galactic chemical evolution.

Key words: molecular data – stars: AGB and post-AGB – stars: carbon – stars: fundamental parameters – stars: Population II – stars: variables: other.

1 INTRODUCTION

Knowledge of stellar population offers a fossil record of the formation and evolution of galaxies and thus provides strong constraints on the scenarios of Galaxy formation and evolution. Carbon stars, for instance, were thought to be giants without exception and were sought as tracers of the outer halo. Recent surveys on stellar populations have led to the discovery of different types of stars, numerous metal-poor stars, carbon and carbon-related objects, etc. (Beers, Preston & Shectman 1992; Totten & Irwin 1998; Beers 1999). One result of these efforts is the major discovery that the fraction of carbon-rich stars increases with decreasing metallicity (Rossi, Beers & Sneden 1999). Extensive analysis of many carbon-enhanced metal-poor stars at high resolution (Norris, Ryan & Beers 1997a,b; Bonifacio et al. 1998; Hill et al. 2000; Norris et al. 2002; Aoki et al. 2000) have revealed many more intriguing results; however, the specific trend of increase in carbon-enhanced stars with decreasing metallicity still remains unexplained. Also, the production mechanisms of carbon in these stars still remain unknown. There are different types of carbon-enhanced stars: (i) stars showing carbon enhancement with s-process element enhancement; (ii) carbon enhancement with r-process element enhancement; and (iii) carbon enhancement with normal n-capture element abundances. There is yet another type of very metal-poor stars with strong s-process enhancement that are only slightly carbon-enhanced ([C/Fe] = +0.2; Hill et al. 2002). Certainly, a single well-defined production mechanism is unlikely to lead to such a diversity in abundances. To shed light on the production mechanisms of carbon excess resulting in different types of carbon-enhanced stars and to understand the nucleosynthesis of s-process and r-process elements at low metallicity, it is desirable to analyse as many different types of carbon-enhanced stars as possible.

Christlieb et al. (2001) reported a sample of 403 faint high-latitude carbon (FHLC) stars identified by means of line indices – i.e. ratios of the mean photographic densities in the carbon molecular absorption features and the continuum bandpasses – which were the basis for the Hamburg catalogue of high Galactic latitude

★E-mail: aruna@iiap.res.in

carbon stars. The identification was primarily based on the presence of strong C_2 and CN molecular bands shortward of 5200 Å; it did not consider CH bands. At high Galactic latitudes, although the surface density of FHLC stars is low, different kinds of carbon stars are known to populate the region (Green et al. 1994). One kind is normal asymptotic giant branch (AGB) stars, carbon-enriched by dredge-up during the post-main-sequence phase, which are found among the N-type carbon stars. Another kind is FHLC stars showing significant proper motions and having the luminosities of a main-sequence dwarf, called dwarf carbon stars (dCs). A third kind of FHLC stars is the so-called CH giant stars, similar to the metal-poor carbon stars found in globular clusters and some dwarf spheroidal (dSph) galaxies (Harding 1962). Among these, at high Galactic latitudes, warm carbon stars (possibly some C-R stars) are also likely to be present. The sample of stars offered by Christlieb et al. (2001), being high-latitude objects, with smaller initial mass and possibly lower metallicity, is likely to contain a mixture of these objects. Different kinds of objects have different astrophysical implications, and hence it is important to distinguish them from one another, although in certain cases it is not easy to do so. For example, dCs are difficult to distinguish from C giants, as they exhibit remarkable similarity in their spectra with those of C giants. They are, however, distinguishable through their relatively high proper motion and apparently anomalous *JHK* infrared colours (Green et al. 1992).

Interpretation of the chemical compositions of the intermediate-mass stars formed from interstellar matter is not straightforward, as the interstellar matter has already been affected by the ejecta of many generations of more massive stars. In comparison, the halo red giant stars offer more direct information on the role of intermediate-mass stars of the halo. Thus, the existence of a CH stellar component has important astrophysical implications for Galactic chemical evolution. The processes responsible for carbon excess in these stars to a large extent are responsible for the origin and evolution of carbon, nitrogen and heavy elements in the early Galaxy. Furthermore, the isotopic ratios of $^{12}C/^{13}C$ in C stars and C-related stars provide useful probes of nucleosynthesis processes and their location leading to carbon excess in these stars. To determine these ratios, useful candidates are those with strong isotopic carbon bands in their spectra; CH stars provide a useful set of candidates.

Determination of the chemical compositions as well as carbon isotopic ratios $^{12}C/^{13}C$ would require high-resolution spectroscopy. Before this, a target list of CH stars needs to be generated, and this can be done from spectral analysis of stars using even low-resolution spectroscopy. Prompted by this we have undertaken to identify the CH as well as other types of stellar objects in the sample of FHLC stars of Christlieb et al. (2001) using low-resolution spectroscopy. These identifications and the low-resolution spectroscopic analysis of the candidate CH stars is the main theme of this paper.

Observations and data reductions are described in Section 2. In Section 3 we briefly discuss different types of C stars and their spectral characteristics. *JHK* photometry of the stars is briefly described in Section 4. A description of the spectra of the programme stars and results are drawn in Section 5. Section 6 contains a brief discussion on the atmospheres of candidate CH stars. Concluding remarks are presented in Section 7.

2 OBSERVATION AND DATA REDUCTION

The stars listed in Table 1 (51 stars) and Table 2 (40 stars) have been observed with the 2-m Himalayan Chandra Telescope (HCT) at the Indian Astronomical Observatory (IAO), Mt. Saraswati, Digparatsa Ri, Hanle, in the period 2003 June–2004 May. The spectra of a number of carbon stars (such as HD 182040, HD 26, HD 5223, HD 209621, Z Psc, V460 Cyg and RV Sct) have also been taken for comparison. The spectrum of the C-R star HD 156074 taken from the atlas of Barnbaum et al. (1996) is also used for comparison. The spectrograph used is the Himalayan Faint Object Spectrograph Camera (HFOSC). HFOSC is an optical imager cum spectrograph for conducting low- and medium-resolution grism spectroscopy.[1] The grism and the camera combination used for observation provided a spectral resolution of $\sim$1330 ($\lambda/\delta\lambda$); the observed bandpass ran from about 3800 to 6800 Å.

Observations of a Th–Ar hollow cathode lamp taken immediately before and after the stellar exposures provided wavelength calibration. The charge-coupled device (CCD) data were reduced using the IRAF software spectroscopic reduction packages. For each object, two spectra each of 15 min exposures were taken and combined to increase the signal-to-noise ratio. 2MASS *JHK* measurements for the stars in Table 1 are also listed. These measurements are available on-line.[2] In Table 2, the objects observed on 2004 March 2 and 3 were acquired using the OMR spectrograph at the Cassegrain focus of the 2.3-m Vainu Bappu Telescope (VBT) at Kavalur. With a 600 line mm^{-1} grating, we get a dispersion of 2.6 Å $pixel^{-1}$. The spectra of these objects cover the wavelength range 4000–6100 Å, at a resolution of $\sim$1000.

3 TYPES OF C STARS AND THEIR SPECTRAL CHARACTERISTICS

Carbon stars are classified into different spectral types based on their characteristic spectral properties. We briefly discuss here the main characteristics essential for our purpose. More detailed discussion on this can be found in the literature, including Wallerstein & Knapp (1998) and references therein. Among the carbon stars, the C-N stars have lower temperatures and stronger molecular bands than those of C-R stars. C-N stars exhibit very strong depression of light in the violet part of the spectrum. They are used as tracers of an intermediate-age population in extragalactic objects. The C-R stars as well as CH stars have warmer temperatures and blue/violet light is accessible to observation and atmospheric analysis. C-N stars are easily detected in infrared surveys from their characteristic infrared colours. The majority of C-N stars show ratios of $^{12}C/^{13}C$ more than 30, ranging to nearly 100, while in C-R stars this ratio ranges from 4 to 9. The strength/weakness of the CH band in C-rich stars provides a measure of the degree of hydrogen deficiency in carbon stars.

The characteristic behaviour of s-process elements in C stars can also be used as a useful indicator of spectral type. The s-process element abundances are nearly solar in C-R stars (Dominy 1984), whereas most of the carbon and carbon-related stars show significantly enhanced abundances of the s-process elements relative to iron (Lambert et al. 1986; Green & Margon 1994).

CH stars are characterized by the strong *G* band of CH in their spectra. These stars are not a homogeneous group of stars. They consist of two populations: the more metal-poor one has a spherical distribution, and the one slightly richer in metals is characterized by a flattened ellipsoidal distribution (Zinn 1985). These stars form a group of warm stars of spectral types equivalent to G and K giants, but show weak metallic lines. The ratio of the local density of CH stars is as high as 30 per cent of metal-poor giants (Hartwick & Cowley 1985). Being the most populous type of halo carbon stars

[1] http://www.iiap.ernet.in/iao/iao.html
[2] http://irsa.ipac.caltech.edu/

Table 1. HE stars with prominent C_2 molecular bands.

Star No.	RA(2000)[a]	Dec.(2000)[a]	l	b	B_J[a]	V[a]	$B-V$[a]	$U-B$[a]	J	H	K	Obs. date
HE 0002+0053	00 05 25.0	+01 10 04	99.71	−59.61	14.5	13.3	1.72	1.25	11.018	10.386	10.118	06.11.04
HE 0017+0055	00 20 21.6	+01 12 07	106.90	−60.70	12.6				9.309	8.693	8.498	15.11.03
HE 0038−0024	00 40 48.2	−00 08 05	117.09	−62.89	15.4	14.4	1.86	1.67	12.433	11.768	11.573	06.11.04
HE 0043−2433	00 45 43.9	−24 16 48	98.33	−86.88	13.8	13.1	1.04	1.00	11.064	10.493	10.365	07.11.04
HE 0110−0406	01 12 37.1	−03 50 30	136.11	−66.17	13.4				10.523	9.988	9.866	17.09.03
HE 0111−1346	01 13 46.5	−13 30 49	145.01	−75.42	13.3				10.684	10.155	10.039	07.11.04
HE 0151−0341	01 53 43.3	−03 27 14	157.78	−62.04	14.6	13.4	1.27	0.87	11.847	11.364	11.248	07.11.04
HE 0207−0211	02 10 12.0	−01 57 39	163.12	−58.55	15.5	14.0	2.16	2.13	11.505	10.605	10.010	07.11.04
HE 0308−1612	03 10 27.1	−16 00 41	201.12	−55.96	12.5				10.027	9.475	9.331	17.09.03
HE 0310+0059	03 12 56.9	+01 11 10	178.95	−45.73	12.6				9.871	9.296	9.196	17.09.03
HE 0314−0143	03 17 22.2	−01 32 37	182.98	−46.69	12.7				8.993	8.222	8.000	17.09.03
HE 0319−0215	03 21 46.3	−02 04 34	184.58	−46.17	14.6	13.6	1.43	1.01	11.785	11.218	11.063	16.09.03
HE 0322−1504	03 24 40.1	−14 54 24	201.90	−52.39	15.0	13.8	1.63	1.24	12.105	11.533	11.340	06.11.04
HE 0429+0232	04 31 53.7	+02 39 01	192.72	−29.17	14.2	13.3	1.35	1.08	11.088	10.520	10.325	07.11.04
HE 0457−1805	04 59 43.6	−18 01 11	217.85	−32.51	12.1	11.2	1.25	1.20	8.937	8.421	8.186	07.11.04
HE 0507−1653	05 09 16.5	−16 50 05	217.54	−29.96	15.6	12.4	1.06	0.68	10.883	10.430	10.315	06.11.04
HE 0518−2322	05 20 35.5	−23 19 14	225.62	−29.74	13.7				11.151	10.672	10.568	15.11.03
HE 0915−0327	09 18 08.2	−03 39 57	235.26	+30.09	14.5	12.9	2.29	2.12	9.968	8.989	8.609	10.04.04
HE 0932−0341	09 35 10.2	−03 54 33	238.38	+33.41	14.8	13.9	1.23	1.02	12.295	11.807	11.708	06.11.04
HE 1008−0636	10 10 37.0	−06 51 13	248.12	+38.35	14.5	12.9	2.28	2.11	9.952	9.073	8.527	29.03.04
HE 1027−2501	10 29 29.5	−25 17 16	266.68	+27.42	13.9	12.7	1.73	1.51				30.03.04
HE 1056−1855	10 59 12.2	−19 11 08	269.48	+36.29	13.6				10.784	10.249	10.090	20.12.04
HE 1104−0957	11 07 19.4	−10 13 16	265.35	+44.92	14.7				8.262	7.561	7.317	20.12.04
HE 1107−2105	11 09 59.6	−21 22 01	273.53	+35.65	14.3	12.1	3.11	2.44	8.279	7.229	6.696	30.03.04
HE 1125−1357	11 27 43.0	−14 13 32	274.20	+43.93	15.2	14.1	1.41	1.40	11.730	11.057	10.842	12.04.04
HE 1145−0002	11 47 59.8	−00 19 19	271.30	+58.60	13.5	13.6	1.48	1.49	10.911	10.240	10.006	11.04.04
HE 1204−0600	12 07 11.6	−06 17 06	283.56	+54.91	14.9	14.0	1.36	1.45	11.517	10.898	10.703	11.04.04
HE 1211−0435	12 14 12.0	−04 52 26	285.83	+56.76	15.0	14.2	1.08	0.90	12.492	11.962	11.916	12.04.04
HE 1228−0402	12 30 50.6	−04 18 59	293.16	+58.16	16.3	15.1	1.68	1.92	12.805	12.070	11.847	11.04.04
HE 1254−1130	12 56 57.0	−11 46 19	305.08	+51.08	16.1	14.5	2.13	2.37	10.731	9.821	9.406	30.03.04
HE 1259−2601	13 01 52.4	−26 17 16	305.84	+36.52	13.9	12.8	1.77	1.56				03.03.04
HE 1304−2046	13 06 50.1	−21 02 10	307.75	+41.69	15.2	14.3	1.32	1.36	11.978	11.386	11.219	30.03.04
HE 1305+0132	13 08 17.8	+01 16 49	312.52	+63.84	13.8	12.8	1.35	1.25	10.621	9.994	9.814	28.03.04
HE 1418+0150	14 21 01.2	+01 37 18	346.80	+56.66	14.2				9.988	9.356	9.127	10.04.04
HE 1425−2052	14 28 39.5	−21 06 05	331.40	+36.64	13.6	12.7	1.27	1.29	10.043	9.446	9.273	28.03.04
HE 1429−0551	14 32 31.3	−06 05 00	343.02	+48.76	13.5				10.734	10.272	10.066	05.09.03
HE 1446−0112	14 49 02.2	−01 25 24	352.42	+49.80	14.5	13.5	1.38	1.39	10.983	10.379	10.162	06.09.03
HE 1501−1500	15 04 26.3	−15 12 00	344.28	+36.78	16.5	15.3	1.65	1.61	12.725	12.030	11.830	10.04.04
HE 1523−1155	15 26 41.0	−12 05 43	351.87	+35.63	14.2	13.4	1.14	0.70	11.372	10.846	10.748	29.03.04
HE 1524−0210	15 26 56.9	−02 20 45	0.98	+42.35	14.4	13.3	1.53	1.25	11.740	11.079	10.896	06.09.03
HE 1528−0409	15 30 54.3	−04 19 40	359.87	+40.30	15.8	15.0	1.10	0.78	12.945	12.455	12.358	29.03.04
HE 2144−1832	21 46 54.7	−18 18 15	34.65	−46.78	12.6				8.768	8.180	7.958	16.09.03
HE 2145−1715	21 48 44.5	−17 01 03	36.63	−46.73	14.2	13.2	1.39	1.18	11.032	10.356	10.255	17.09.03
HE 2207−0930	22 09 57.5	−09 16 06	50.27	−47.96	14.4	13.1	1.82	1.40	10.527	9.812	9.607	16.09.03
HE 2207−1746	22 10 37.5	−17 31 38	38.87	−51.77	11.8				9.115	8.579	8.450	06.09.03
HE 2218+0127	22 21 26.1	+01 42 20	65.46	−43.80	14.6	14.0	0.80	0.31	11.826	11.509	11.433	16.09.03
HE 2221−0453	22 24 25.7	−04 38 02	59.04	−48.38	14.7	13.7	1.36	1.11	11.524	10.997	10.815	17.09.03
HE 2239−0610	22 41 53.1	−05 54 22	61.61	−52.61	14.1	13.1	1.34	1.59	13.830	13.296	13.164	07.11.04
HE 2319−1534	23 22 11.1	−15 18 16	58.09	−66.14	15.3	13.8	2.09	2.16	10.866	9.937	9.367	17.09.03
HE 2331−1329	23 33 44.5	−13 12 34	66.55	−67.12	16.2	14.5	2.29	2.19	11.841	10.990	10.652	06.11.04
HE 2339−0837	23 41 59.9	−08 21 19	78.51	−65.05	14.9	14.0	1.32	0.62	12.632	12.107	12.026	06.11.04

[a]From Christlieb et al. (2001).

known, CH stars are important objects for our understanding of Galactic chemical evolution, the evolution of low-mass stars and nucleosynthesis in metal-poor stars.

Most of the CH stars are known to be high-velocity objects. 'CH-like' stars, where CH are less dominant, have low space velocities (Yamashita 1975). At low resolution, to make a distinction between CH and C-R stars is difficult, as many C-R stars also show quite a strong CH band. In such cases, the secondary P-branch head near 4342 Å is used as a more useful indicator. Another important feature is the strength of Ca I at 4226 Å, which in the case of CH stars is weakened by the overlying faint bands of the CH band systems. In C-R stars, this feature is quite strong. These spectral

Table 2. HE stars without prominent C_2 bands.

Star No.	RA(2000)[a]	Dec.(2000)[a]	l	b	B^a	V^a	$B-V^a$	$U-B^a$	Bands noticed	Obs. date
HE 0201−0327	02 03 49.0	−03 13 05	161.94	−60.49	14.1	13.4	1.02	0.95	CH, CN	07.11.04
HE 0333−1819	03 35 18.8	−18 09 54	208.37	−51.32	12.6				CH, CN	16.09.03
HE 0359−0141	04 02 21.2	−01 33 05	192.03	−37.64	14.5	13.4	1.26	1.08	CH, CN	15.11.03
HE 0408−1733	04 11 06.0	−17 25 40	211.87	−43.11	13.1	12.2	1.28	1.26	CH, CN	17.09.03
HE 0417−0513	04 19 46.8	−05 06 17	198.66	−35.82	14.6	13.7	1.31	1.21	CH, CN	15.11.03
HE 0419+0124	04 21 40.4	+01 31 46	192.17	−31.92	15.7	13.0	1.44	1.37	CH, CN	07.11.04
HE 0443−1847	04 46 10.9	−18 41 40	217.23	−35.75	13.1	12.9	1.27	1.21	CH, CN	16.09.03
HE 0458−1754	05 00 34.5	−17 50 21	217.73	−32.26	13.5	12.7	1.18	1.09	CH, CN	02.03.04
HE 0508−1604	05 10 47.0	−16 00 40	216.82	−29.31	12.8	12.1	1.04	1.15	CH, CN,	20.12.04
HE 0518−1751	05 20 28.4	−17 48 43	219.71	−27.84	13.5	12.8	1.05	1.22	CH, CN	07.11.04
HE 0519−2053	05 21 54.4	−20 50 36	223.06	−28.62	13.6	13.7	1.18	1.14	CH, CN	15.11.03
HE 0536−4257	05 37 40.4	−42 55 39	248.71	−31.11	13.8	12.7	1.44	1.41		03.03.04
HE 0541−5327	05 42 14.3	−53 26 31	261.05	−31.59	13.6					03.03.04
HE 0549−4354	05 50 34.3	−43 53 24	250.28	−28.98	13.7	12.8	1.31	1.18	CH	03.03.04
HE 0900−0038	09 02 50.5	−00 50 20	230.15	+28.43	14.2	13.3	1.27	1.19	CH, CN	29.03.04
HE 0916−0037	09 18 47.6	−00 50 35	232.63	+31.79	13.7	12.8	1.24	1.02	CH	03.03.04
HE 0918+0136	09 21 26.1	+01 23 28	230.81	+33.55	14.0	13.1	1.30	1.21	CH	03.03.04
HE 0919+0200	09 22 13.0	+01 47 56	230.52	+33.93	13.5	12.6	1.31	1.20	CH	03.03.04
HE 0930−0018	09 33 24.7	−00 31 46	234.74	+35.01	14.2	14.7	1.43	1.45	CH	02.03.04
HE 0935−0145	09 37 59.0	−01 58 36	236.99	+35.12	13.8	12.9	1.16	1.07	CH	02.03.04
HE 0939−0725	09 42 11.9	−07 39 06	243.19	+32.50	14.0	13.1	1.20	1.13	CH, CN,	20.12.04
HE 1042−2659	10 44 24.2	−27 15 30	271.05	+27.64	14.7	12.6			CH	03.03.04
HE 1117−2304	11 19 42.8	−23 21 07	277.08	+34.87	13.3				CH, CN	11.04.04
HE 1119−3229	11 22 21.9	−32 46 19	282.08	+26.47	14.0	13.1	1.18	1.25	CH	03.03.04
HE 1227−3103	12 30 34.5	−31 19 54	297.72	+31.33	14.3	13.3	1.39	1.54		02.03.04
HE 1304−3020	13 07 24.2	−30 36 36	306.99	+32.14	13.5	12.7	1.17	1.06	CH	02.03.04
HE 1356−2752	13 59 25.0	−28 06 59	320.71	+32.40	13.3				CH	03.03.04
HE 1455−1413	14 57 51.6	−14 25 10	343.27	+38.36	13.1				CH	03.03.04
HE 1500−1101	15 03 40.9	−11 13 09	347.25	+40.01	13.8	12.9	1.28	1.24	CH	29.03.04
HE 1514−0207	15 16 38.9	−02 18 33	358.67	+44.29	13.6				CH, CN	05.09.03
HE 1521−0522	15 24 12.2	−05 32 52	357.20	+40.70	14.7	13.8	1.24	1.11	CH, CN	11.04.04
HE 1527−0412	15 29 42.3	−04 22 22	369.56	+40.49	13.8	12.9	1.21	1.19	CH, CN	05.09.03
HE 2115−0522	21 18 11.8	−05 10 07	46.39	−34.80	17.4	14.3	1.22	1.15	CH, CN	07.11.04
HE 2121−0313	21 23 46.2	−03 00 51	49.51	−34.90	14.9	13.9	1.35	1.47	CH, CN	05.09.03
HE 2124−0408	21 27 06.8	−03 55 22	49.09	−36.09	14.8	13.9	1.26	1.15	CH, CN	17.09.03
HE 2138−1616	21 41 16.6	−16 02 40	36.95	−44.70	14.7	13.9	1.01	0.91	CH, CN	16.09.03
HE 2141−1441	21 44 25.7	−14 27 33	39.43	−44.77	14.3	13.5	1.13	1.03	CH, CN	16.09.03
HE 2145−0141	21 47 48.3	−01 27 50	55.23	−39.10	13.4	12.6	1.10	1.02	CH, CN	16.09.03
HE 2224−0330	22 26 47.9	−03 14 58	61.23	−48.01	14.3	13.5	1.08	0.94	CH, CN	16.09.03
HE 2352−1906	23 54 49.0	−18 49 31	62.50	−74.57	12.9				CH, CN	16.09.03

[a]From Christlieb et al. (2001).

characteristics allow for an identification of CH and C-R stars even at low resolution. Enhanced lines of s-process elements, weaker Fe-group elements as well as various strengths of C_2 bands are some of the other distinguishing spectral features of CH stars. However, at low dispersion the narrow lines are difficult to estimate and essentially do not provide a strong clue to distinguish C-R stars from CH stars. Although CH and C-R stars have similar ranges of temperatures, the distribution of CH stars places most of them in the Galactic halo: their large radial velocities, typically ∼200 km s^{-1}, are indicative of their being halo objects (McClure 1983, 1984).

The objects observed from Hanle are classified considering these spectral characteristics. In the following we discuss the medium-resolution spectra of the objects listed in Table 1 with their photometric data.

4 *JHK* PHOTOMETRY

Infrared colours made from *JHK* photometry provide a supplementary diagnostic for stellar classification. Fig. 1 is a two-colour *JHK* diagram in which the $(J-H)$ versus $(H-K)$ colours of the HE stars listed in Table 1 are plotted. The 2MASS *JHK* measurements of the HE stars are available on-line.[3]

The two boxes superimposed in the figure, representing the location of CH stars (thick box, lower left) and C-N stars (thin box, upper right), illustrate the loci of the separate carbon star types and are taken from Totten et al. (2000). In this figure, the CH stars classified by us (following our discussions in the subsequent sections),

[3] http://iras.ipac.caltech.edu/

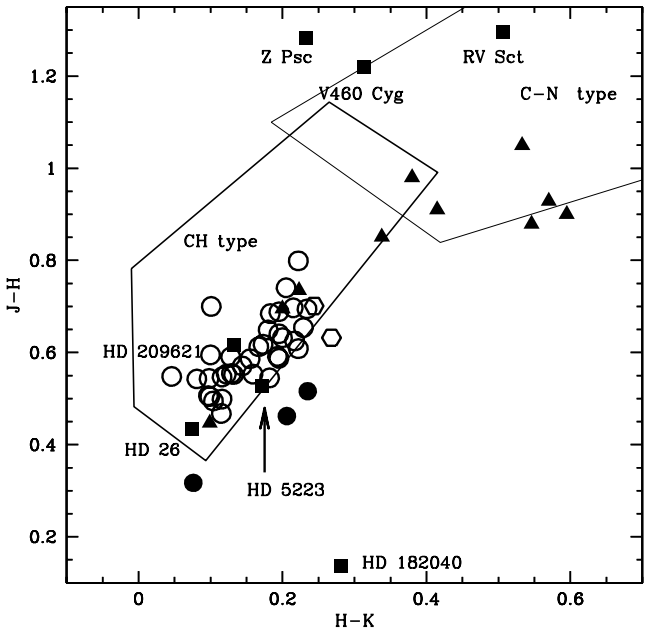

Figure 1. A two-colour ($J - H$) versus ($H - K$) diagram of the stars listed in Table 1. The candidate CH stars are represented by open circles except for the three outliers represented by solid circles. C-N stars are represented by solid triangles and C-R stars by open hexagons. The two boxes superimposed in the figure illustrate the loci of separate carbon star types and are taken from Totten et al. (2000). The location of the comparison stars are labelled and marked with solid squares.

plotted with open circles, fall well within the CH box, except for the three outliers HE 1429−0551, 2218+0127 and 0457−1805, represented by solid circles. The spectral characteristics of these stars led us to classify them as CH stars. Their spectra do not show any peculiarities from which their location in the ($J - H$) versus ($H - K$) plane seems obvious. A difference between the spectra of the first two stars lies in molecular C_2 bands in the spectral region 5700–6800 Å. In this region HE 1429−0551 does not show molecular C_2 bands (or could be marginally detected) whereas HE 2218+0127 shows molecular C_2 bands as strongly as (or marginally stronger than) they are seen in the CH star HD 5223. The Ba II feature at 6496 Å is weak in HE 1429−0551. In HE 2218+0127, this feature appears to be of equal depth to its counterpart in HD 5223. Also, HE 2218+0127 seems to be the warmest among the candidate CH stars (Table 3). HE 0457−1805, another CH star outside the CH box, resembling HD 26, a known CH star, shows a stronger CN molecular band around 4215 Å and slightly stronger features due to Ba II at 6496 Å and Na I D. The Hα feature is marginally weaker but the *G* band of CH appears almost of equal strength. There are 10 stars in the present sample that show the spectral characteristics of C-N stars, represented by solid triangles in Fig. 1. Four of them fall well within the C-N box, three of them just outside the C-N box, and the remaining two within the CH box. Stars HE 2319−1534 and 1008−0636 at the redder edge of the C-N box show Hα and Hβ in emission, whereas HE 2331−1329, 0915−0327 and 1254−1130 with lower ($H - K$) values do not show Hα and Hβ features in their spectra. HE 1501−1500, 1228−0402 and 1107−2005 (inside the CH box) do not have any flux below 4500 Å. The CN molecular bands are weaker in HE 1228−0402 than their counterparts in other C-N stars. This is not the case with HE 1501−1500. No Hα and Hβ features are detectable in these last two stars. At present it remains to be understood why these two stars occupy a location among the CH stars in the ($J - H$) versus ($H - K$) plane.

5 RESULTS

5.1 Spectral characteristics of the programme stars

The spectra are examined in terms of the following spectral characteristics:

(1) strength (band depth) of the CH band around 4300 Å;
(2) prominence of secondary P-branch head near 4342 Å;
(3) strength/weakness of the Ca I feature at 4226 Å;
(4) isotopic band depths of C_2 and CN, in particular the Swan bands of $^{12}C^{13}C$ and $^{13}C^{13}C$ near 4700 Å;
(5) strength of other C_2 bands in the 6000–6200 Å region;
(6) ^{13}CN band near 6360 Å and other CN bands across the wavelength range;
(7) strength of s-process elements such as Ba II features at 4554 and 6496 Å.

To establish the membership of a star in a particular group, we have conducted a differential analysis of the spectra of the programme stars with the spectra of carbon stars available in the low-resolution spectral atlas of carbon stars of Barnbaum, Stone & Keenan (1996). We have also acquired spectra for some of the objects from this atlas and used them for comparison of spectra at the same resolution.

5.2 Candidate CH stars: description of the spectra

5.2.1 A comparison of known C-R and CH star spectra

At low resolution, the spectra of C-R and CH stars look very similar, and this makes distinction between them a difficult task. The differences are made apparent by making a comparison between spectra of known C-R and CH stars. Application of this comparison to the programme stars helped in an easy identification of their spectral class. In Figs 2 and 3 we show a comparison of the spectra of a pair of C-R stars, HD 156074 and 76846, and a pair of CH stars, HD 209621 and 5223. Although we have considered four stars here, the comparison is generally true for any C-R and CH stars.

(i) *Wavelength region 4000–5400 Å (Fig. 2).* The *G* band of CH is strong in all the spectra, almost of equal strength. However, the secondary P-branch head around 4342 Å is distinctly seen in the CH star spectra. In C-R star spectra this feature is merged with contributions from molecular bands. In C-R stars the Ca I at 4226 Å line depth is almost equal to the CN band depth at 4215 Å, whereas in CH star spectra this line is marginally noticed. The CN band around 4215 Å is much deeper in C-R stars than in the CH stars. Narrow atomic lines are blended with contributions from molecular bands and hence their real strength could not be estimated at this resolution. In the above wavelength range, Hβ and Ba II at 4554 Å are the two features clearly noticeable in the CH stars. In C-R stars this region is a complex combination of atomic and molecular lines. There is no obvious distinction in the isotopic bands around 4700 Å in C-R and CH stars. The C_2 molecular bands around 5165 and 5635 Å are two prominent features in this region.

(ii) *Wavelength region 5400–6800 Å (Fig. 3).* The C_2 molecular band around 5635 Å is the most prominent feature in this region. This region too is a complex mixture of atomic and molecular lines. The blended feature of Na I D_1 and Na I D_2 in C-R stars is sharper with two distinct dips. In CH stars this feature is shallower and the

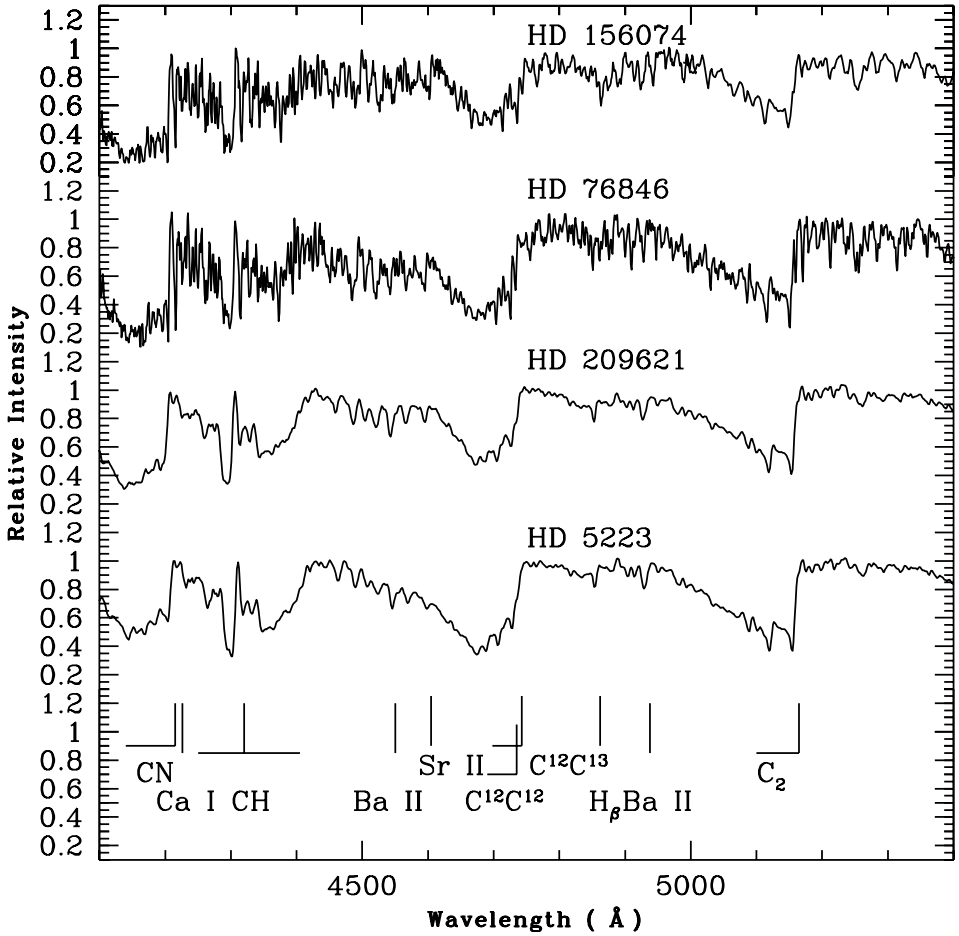

Figure 2. A comparison of the spectra of the pair of C-R stars HD 156074 and 76846 and the pair of CH stars HD 5223 and 209621 in the wavelength region 4100–5400 Å. The most prominent features noticeable are marked on the figure.

individual contributions of Na I D_1 and Na I D_2 are not distinguishable. The Hα feature appears as a distinct feature in CH stars; in C-R stars this feature seems to be contaminated by molecular contributions. The Ba II feature at 6496 Å is also blended with contributions from CN bands around 6500 Å; in CH stars this blending is not so severe. CN molecular bands, although present, are in general weaker in CH stars than in C-R stars.

The main features of the above comparison are used to identify the spectral type (CH or C-R) of the programme stars. A small number of C-N stars were easily identified from their distinct spectral properties. In Fig. 4 we present the spectra of the comparison stars in the wavelength region 4000–6800 Å. In Fig. 5 we show one example of HE stars corresponding to each comparison star's spectrum in Fig. 4, in the sequence top to bottom. In the following, we present the spectral description of the individual stars.

5.2.2 Spectral description of individual stars

HE 2145−1715, 0518−2322, 0457−1805, 0043−2433 and 1056−1855. The spectra of these objects closely resemble the spectrum of HD 26, a known CH star. The CH bands around λ4300 are of almost equal strength in the spectra of these stars. The Ca I 4226 Å line is very weak, and the Fe I λ4271 line is barely detectable. The strengths of the *G* band of CH, the prominent secondary P-branch head around 4342 Å and the weak Ca I feature at 4226 Å show that these stars could be CH stars.

The C_2 molecular bands around 4730, 5165 and 5635 Å are much deeper in HE 2145−1715 than their counterparts in HD 26. The Hβ features are of equal strength. The Ba II line around 4545 Å is marginally weaker in the spectrum of HE 2145−1715, whereas the Ba II feature at 6496 Å and Hα are of equal strength. The effective temperature of HD 26 is ∼4880 K, and [Fe/H] = −0.5 (Aoki & Tsuji 1997). A marginally weaker Na I D feature than in the HD 26 spectrum and the deeper C_2 bands in HE 2145−1715 are perhaps an indication of slightly lower metallicity and lower temperature for HE 2145−1715 than HD 26. This statement however can only be confirmed from high-resolution spectral analysis.

In HE 0518−2322, the CN molecular band depth matches well with that of HD 26. Na I D appears weakly in emission, and Ba II at 6496 Å and Hα features are marginally stronger. The Hα feature has a weak emission at the absorption core. HE 0043−2433 has a stronger CN band around 4215 Å, but Hα, Hβ and Ba II at 6496 Å appear with almost similar strength to those in HD 26. The Na I D feature appears weakly in absorption in this star. In HE 0457−1805, Na I D is stronger than in HD 26 but Hα, Hβ and Ba II at 6496 Å appear with almost similar strength. In HE 1056−1855, Hα and Hβ are marginally weaker but Ba II at 6496 Å appears with almost equal strength as in HD 26.

HE 0310+0059, 2239−0610, 0932−0341 and 0429+0232. The spectra of these four stars resemble the spectrum of HD 26 to a large

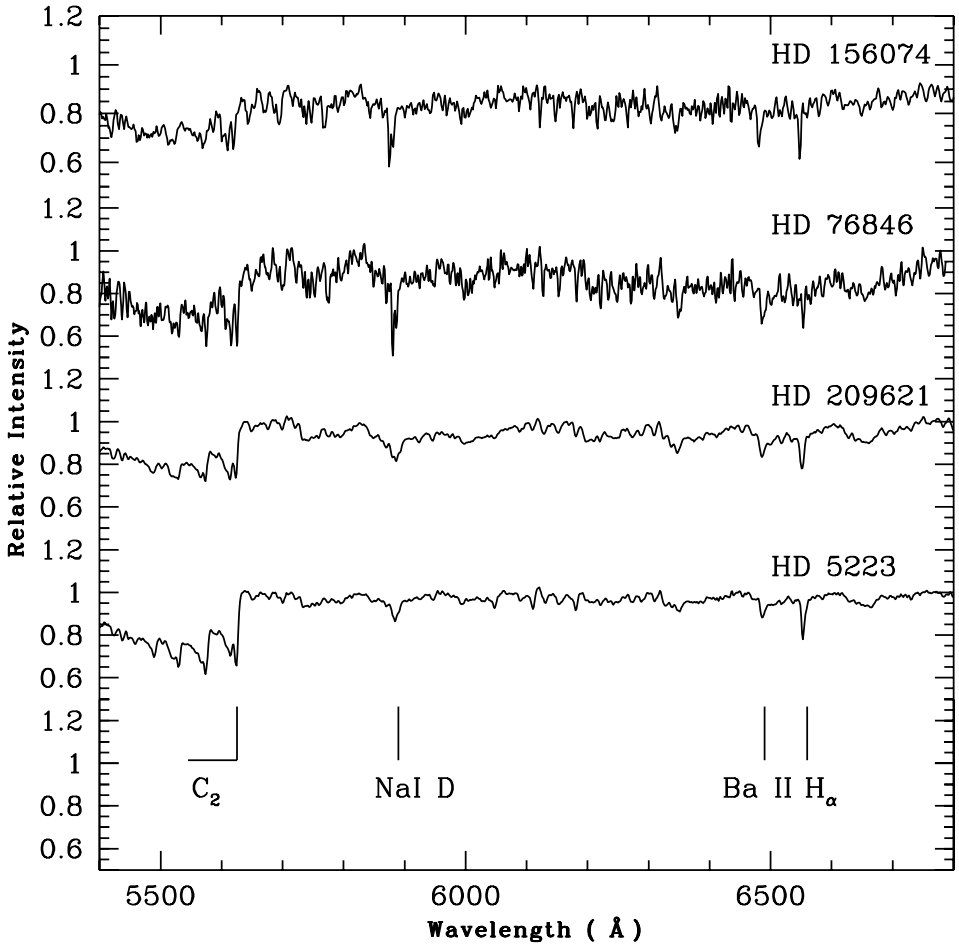

Figure 3. Same as Fig. 2 but for the wavelength region 5400–6800 Å. The prominent features of Na I D, Ba II at 6496 Å, Hα and C_2 molecular bands around 5635 Å are indicated.

extent. The *G*-band of CH around 4300 Å is of similar strength to that in HD 26, but the secondary P-branch head around 4342 Å is not seen as prominently as it is in CH stars. Further, in contrast to HD 26, these stars exhibit a strong Ca I feature at 4226 Å in their spectra. These stars do not seem to be potential candidate CH stars. In HE 0310+0059, lines appear much sharper than in HD 26, and especially the Na I D feature is seen as a much stronger feature in absorption. In HE 0429+0232, this feature is marginally weaker than in HD 26. In HE 2239−0610 and 0932−0341, the Na I D features appear in weak emission. The CN bands are stronger in HE 0310+0059 but the C_2 bands are of similar strength. The Hα, Hβ and Ba II feature at 6496 Å appear in these stars almost with equal strength as in HD 26.

HE 0110−0406, 0308−1612, 0314−0143, 1125−1357, 1211−0435, 1425−2052, 1446−0112, 1524−0210, 1528−0409, 2144−1832 and 2207−1746. The spectra of these stars closely resemble the spectrum of HD 209621 except for some marginal differences in the molecular band depths. The star HD 209621 is a known CH giant with effective temperature ∼4700 K and metallicity −0.9 (Wallerstein 1969; Aoki & Tsuji 1997).

Except for HE 1446−0112 and 1524−0210, the CN band depth around λ4215 are weaker in the programme stars' spectra than in the spectrum of HD 209621. Ca I at 4226 Å is not detectable in the spectra of HE 1446−0112, 1127−1357 and 1211−0435, but appears weakly in the spectra of the rest of the stars. In the first three stars, although the Ca I feature at 4226 Å is seen with a depth almost half the depth of the CN band around 4215 Å, it should be noted that in these three stars the CN band itself is much weaker than its counterpart in HD 209621 and in C-R stars. The CH band at λ4300 in the spectra of the programme stars is equal to or stronger than in the spectrum of HD 209621, except for HE 2207−1746, 0308−1612 and 0110−0406, where this feature is slightly weaker. In these stars the CN band around 4215 Å is also weak, much weaker than in C-R stars. The secondary P-branch head around 4342 Å is seen prominently in all the cases. We assign these stars to the CH group. The molecular bandhead of C_2 around λ4700 is of equal strength in HE 1446−0112, 1524−0210 and 1127−1357; in the rest of the stars this band is slightly weaker than in HD 209621. The C_2 band depths around λ5165 and λ5635 are almost of equal strength, except for stars HE 2207−1746, 1211−0435, 0308−1612 and 0110−0406. The Ba II feature at 4554 Å is detectable and of similar strength; however, the Hβ feature is weaker in HE 1524−0210 and 1528−0409. Except in HE 1446−0112 and 1528−0409, where the Na I D feature appears slightly weaker, in the spectra of the rest of the stars this feature is of similar strength to that of the Na I D feature in HD 209621. The Ba II feature at 6496 Å, which is seen distinctly in HD 209621, appears blended with the CN molecular band in HE 1446−0112. In HE 1125−1357, 1528−0409 and 1211−0435, this feature appears slightly weaker than in HD 209621 and in the rest they seem to be of equal strength. The Hα profile is of equal strength

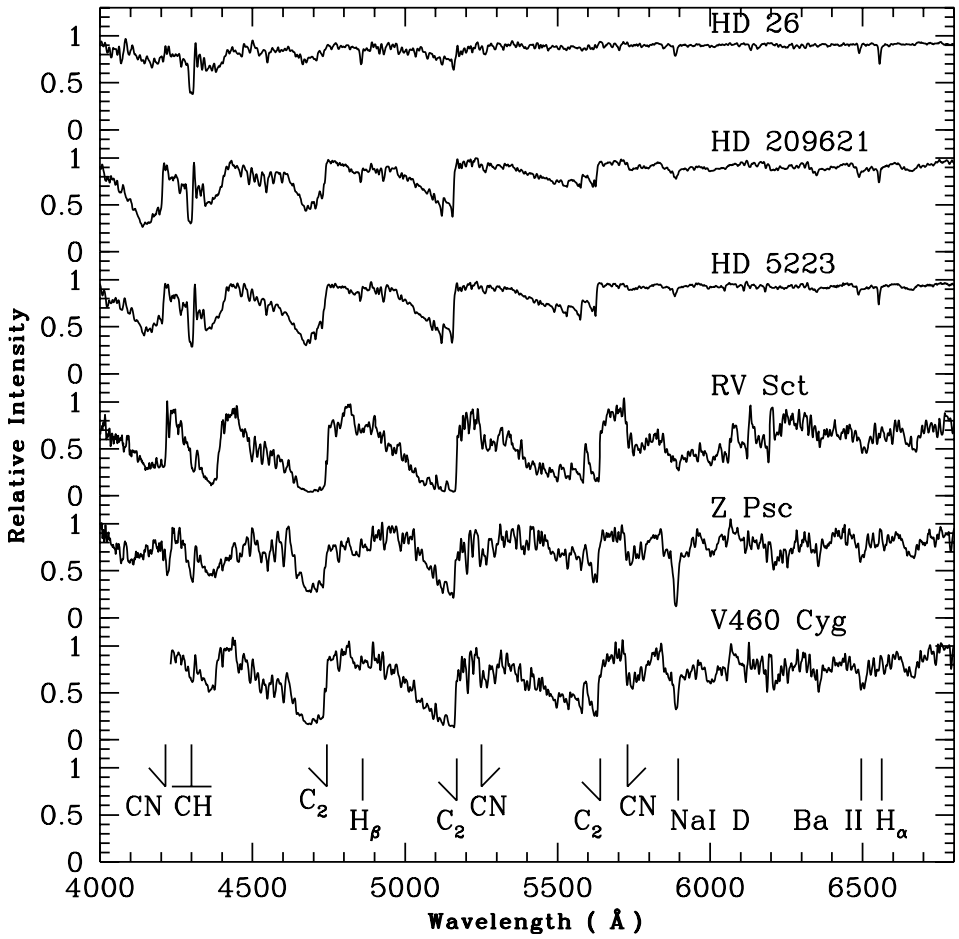

Figure 4. The spectra of the comparison stars in the wavelength region 4000–6800 Å.

in all the stars except HE 0314−0143, where this feature is slightly weaker. In Fig. 6, we show as an example a comparison of the spectra of three objects in the wavelength region 4125–5400 Å with the spectrum of HD 209621.

HE 1429−0551, 1523−1155, 2218+0127, 2221−0453, 1204−0600, 1418+0150, 2207−0930, 1145−0002, 0111−1346, 0151−0341, 0507−1653, 0038−0024, 0322−1504 and 2339−0837. With marginal differences in the molecular band depths, the spectra of these stars closely resemble the spectrum of HD 5223, a well-known CH giant with effective temperature ∼4500 K, and metallicity −1.3 (Aoki & Tsuji 1997).

The CN band depth around λ4215 in these HE stars is very similar to the CN band depth in the spectrum of HD 5223 except for HE 1145−0002, where this feature is weaker and does not show a sharp clear bandhead. The *G* band of CH around λ4300 in the spectra of the programme stars closely resembles its counterpart in HD 5223. Ca I at 4226 Å is seen in the spectra of HE 2218+0127, 1204−0600 and 2207−0930 but not as prominently as in C-R stars. Moreover, the line depth of this feature is quite shallow compared to the CN molecular band depth around 4215 Å. We note that in C-R stars these two features appear with almost equal depth and the CN band depth is deeper in C-R stars than in CH stars.

The Ca I feature is seen marginally also in the rest of these spectra. Fe I at 4271.6 Å, although weak, could be marginally detected in all the spectra. The prominence of the secondary P-branch head near 4342 Å, the strong *G* band of CH and the weak or marginally detectable Ca I feature at 4226 Å allow these stars to be placed in the CH group. The dominance of CH is shown not only by the marked band depths, but also by the weakness of Ca I at 4226 Å and distortion of metallic lines between 4200 and 4300 Å. In Fig. 7, we show a comparison of three spectra in the wavelength region 4000–5400 Å with the spectrum of HD 5223.

Isotopic bands of the Swan system around λ4700 appear to be of equal strength in HE 1204−0600 and 2218+0127 with their counterpart in HD 5223. These bands are slightly deeper in HE 2207−0930, 1145−0002 and 2221−0453 and marginally shallower in HE 1429−0551 and 1523−1155. The C_2 bands around λ5165 and λ5635 closely resemble those in the spectrum of HD 5223, except for stars HE 2207−0930 and 1145−0002, where these bands are slightly deeper. As in the case of HD 5223, the Ba II feature at 4554 Å is seen distinctly in the spectra of the programme stars. However, in HE 1429−0551, 1523−1155 and 2218+0127 this feature is marginally weaker, and in the rest the feature is of similar strength. The Hβ feature appears in all the spectra with similar strength as in HD 5223. Except in HE 1429−0551, 1523−1155 and 2121−0453, the Na I D feature appears slightly stronger as compared to this feature in HD 5223. The Ba II feature at 6496 Å appears weaker in HE 1429−0551, 1523−1155 and 2218−0127 than in HD 5223; this feature appears blended with contributions from CN molecular bands in HE 1204−0600, 2207−0930 and 1145−0002. The Hα profile is of equal strength in HE 1429−0551, 1523−1155, 2218−0127 and 2221−0453; this feature appears slightly weaker in HE 1204−0600, 2207−0930 and 1145−0002 and blended with

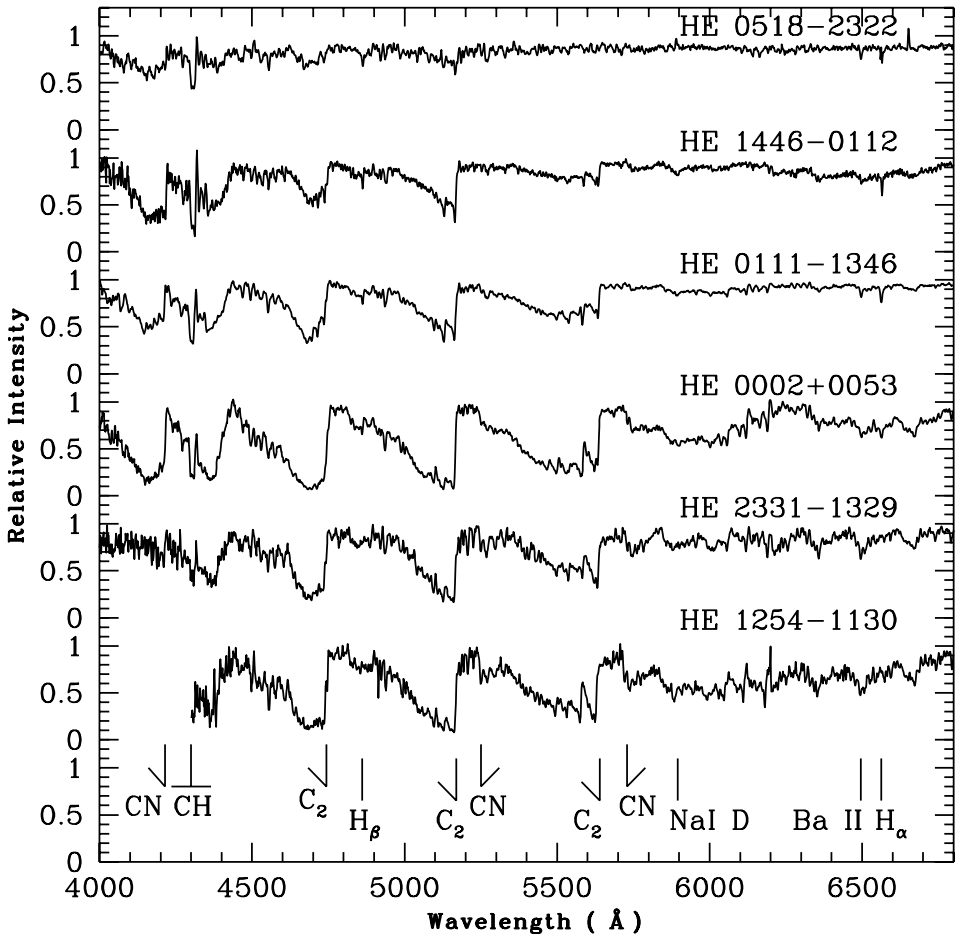

Figure 5. One example of each of the HE stars corresponding to the comparison stars presented in Fig. 4, in the top to bottom sequence, in the wavelength region 4000–6800 Å. The locations of some prominent features seen in the spectra are marked on the figure. HE 1254−1130 has low flux below about 4400 Å. The Ba II at 6496 Å and Hα features seen in the top three spectra are not detectable in the lower three spectra. Except for the Na I D feature, which is barely detectable in the spectra of HE 2331−1329 and 1254−1130, these two spectra closely resemble the spectra of their comparison stars, Z Psc and V460 Cyg, respectively.

contributions from molecular bands. The spectra of HE 1204−0600, 2207−0930 and 1145−0002 closely resemble the spectrum of HD 5223 in the wavelength region 4000–5800 Å; they show marginally stronger CN bands in the wavelength region 5700–6800 Å.

The spectra of HE 0111−1346 and 0322−1504 show a very good match with the spectrum of HD 5223, with similar depths in molecular bands, and also the line depths of Hα, Hβ and Ba II at 6496 Å appear with similar strength. In HE 0322−1504, Na I D appears weakly in emission.

In HE 0151−0341, the *G* band of CH around 4300 Å and the CN band around 4215 Å have similar strength, but the C_2 bands are marginally weaker than in HD 5223. Hα and Hβ are of equal strength, but Na I D and Ba II at 6496 Å are much weaker than in HD 5223. HE 0507−1653 has marginally weaker bands and also the Na I D feature is slightly weaker than in HD 5223; Hα, Hβ and Ba II at 6496 Å appear with similar strength. The spectra of HE 0038−0024 and 2339−0837 show a marginally stronger CN band around 4215 Å and *G* band of CH around 4300 Å, but exhibit slightly weaker C_2 molecular bands. The Na I D feature appears in weak emission, Hα is of similar strength, and Ba II at 6496 Å appears in equal strength in HE 0038−0024, but is marginally weaker in HE 2339−0837.

HE 1305+0132, 1027−2501, 1304−2046, 0017+0055 and 0319−0215. The spectra of these stars also show spectral characteristics of CH stars. The spectra exhibit a strong *G* band of CH. The secondary P-branch head of CH near 4342 Å is seen distinctly, as usual in CH star spectra. The Ca I feature at 4226 Å is weak or undetectable in their spectra. We place these stars in the CH group. Ba II at 4554 Å, Sr II around 4606 Å and Hβ are seen in their spectra. Strong molecular bands include C_2 Swan bands around 4700 Å and C_2 bands around 5165 and 5635 Å. The Ba II feature around 6496 Å is blended with contributions from CN bands. The CN bands around 5730 and 6300 Å are detected. Na I D features appear very similar as seen in most of the CH stars except HE 0319−0215, where this feature appears in weak emission.

5.3 Candidate C-N stars: description of the spectra

HE 2319−1534, 1008−0636, 2331−1329, 0207−0211 and 1107−2105. The spectra of these stars show a close resemblance with the spectrum of C-N star Z Psc with similar strengths of CN and C_2 bands across the wavelength regions. In Fig. 8, we show, as an example, a comparison of spectra for three objects in the wavelength region 5500–6800 Å with the spectrum of Z Psc. The

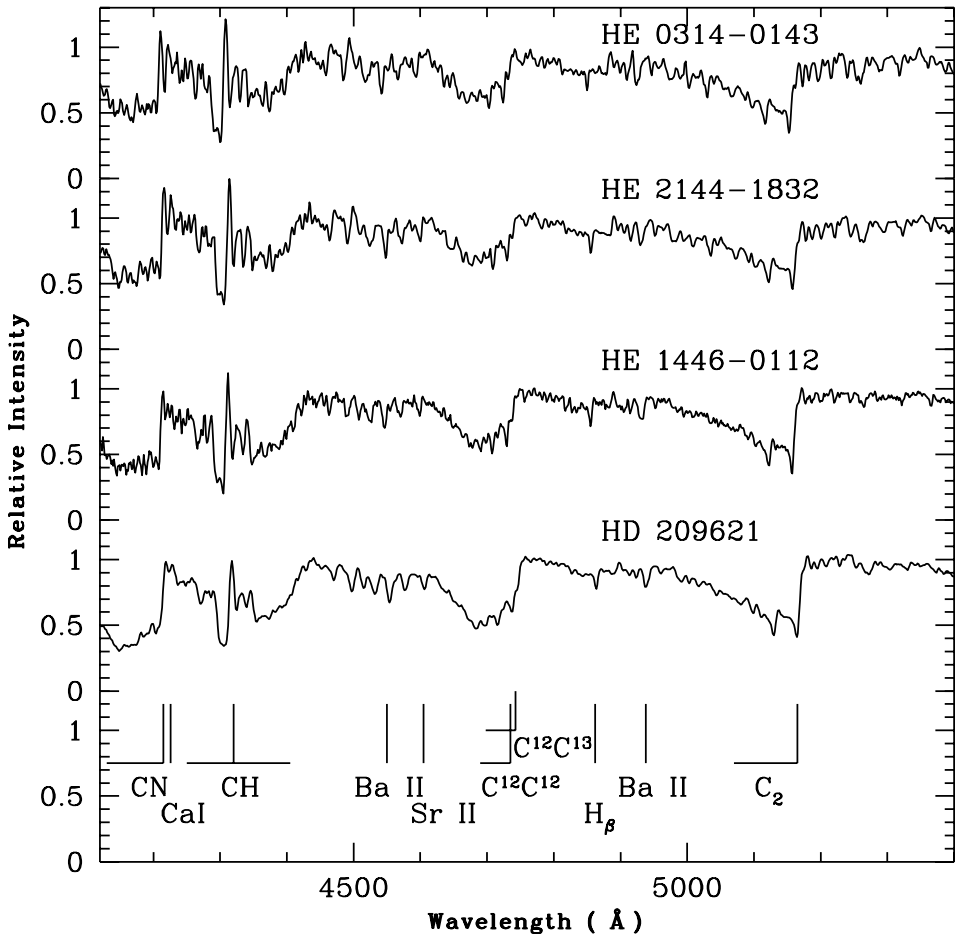

Figure 6. A comparison of the spectra of three HE stars in the wavelength region 4120–5400 Å with the spectrum of the comparison star HD 209621. Prominent features seen in the spectra are marked on the figure.

spectra of HE 2319−1534, 1008−0636 and 1107−2105 have low flux below about 4500 Å. In HE 1008−0636 the SiC_2 bands around 4800–5000 Å are seen. These red-degraded features are not seen in the other four and Z Psc. The Na I D feature is much deeper in HE 1008−0636 than in HE 2319−1534. In the spectrum of HE 2331−1329, the Ca I feature at 4226 Å is much weaker than in Z Psc. The *G* band of CH around 4300 Å and C_2 molecular bands are of similar strength, but the CN bands are much weaker in HE 2331−1329 than their counterparts in Z Psc. The Na I D, Hα and Hβ features are marginally detectable in this star. In HE 0207−0211 the CN bands are much weaker than in Z Psc but the C_2 bands are a good match; Na I D is weak and barely detectable. In HE 0207−0211 and 1107−2105, Hα and Hβ appear in emission; these two features are also seen strongly in emission in the spectra of HE 2319−1534 and 1008−0636, indicative of a possible strong chromospheric activity or shock waves of the type associated with Mira variables.

HE 1228−0402, 0915−0327, 1254−1130, 1501−1500 and 1259−2601. The spectra of these stars show very low flux below about 4500 Å. Their spectra mostly resemble the spectra of C-N stars, with prominent CN and C_2 bands seen across the wavelength range. The spectrum of the C-N star V460 Cyg compares closest to the spectra of these stars. The Na I D feature is weaker in their spectra as compared to their counterparts in V460 Cyg. We place these stars in the C-N group. In V460 Cyg the molecular bands of C_2 as well as CN are much deeper than in Z Psc.

HE 0002+0053 and 1104−0957. The spectra of these two objects closely resemble the spectrum of the C-R star RV Sct. The C_2 bands in the spectrum of HE 0002+0053 match closely with those in RV Sct, but the CN bands are much weaker. In HE 1104−0957 the molecular bands due to both CN and C_2 are much weaker than those in RV Sct. In both the stars, Hα and Hβ are weakly seen in absorption. Na I D is marginally detectable but weaker than in RV Sct. The *G* band of CH around 4300 Å is marginally stronger in these stars. The Ca I feature around 4226 Å, which appears weakly in the spectrum of RV Sct, is missing in the spectra of these two stars. The ^{13}C isotopic band around 4700 Å is absent in these two stars. The CN band around 5200 and 5700 Å seen distinctly in RV Sct is marginally detected in HE 0002−0053, but not seen in HE 1104−0957.

6 ATMOSPHERES OF CH STARS

6.1 Effective temperature

Preliminary estimates of the effective temperatures of the candidate CH stars are determined by using a temperature calibration derived by Alonso et al. (1996). This calibration was derived by using a large number of lower main-sequence stars and subgiants, whose temperatures were measured by the infrared flux method, and holds within temperature and metallicity ranges of $4000 \leqslant T_{\rm eff}/{\rm K} \leqslant 7000$ and $-2.5 \leqslant {\rm [Fe/H]} \leqslant 0$. This calibration relates $T_{\rm eff}$ with Strömgren indices as well as [Fe/H] and colours $(V-B)$, $(V-K)$,

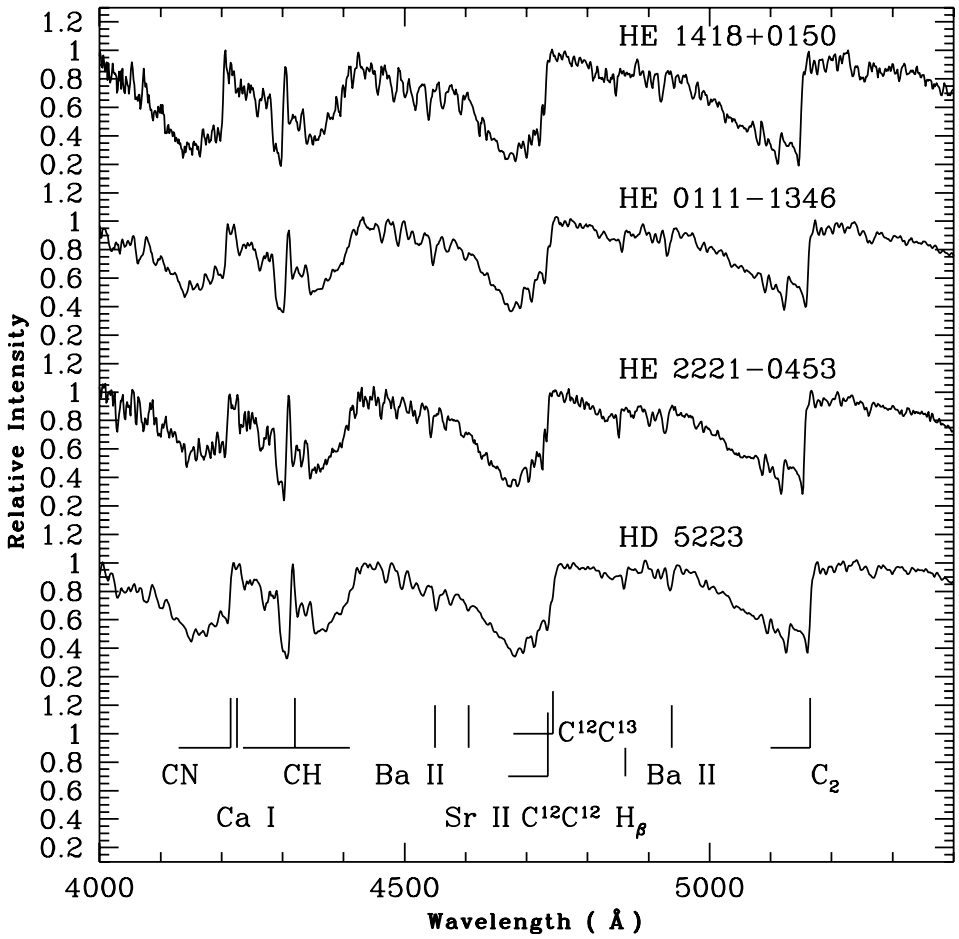

Figure 7. A comparison of the spectra of three HE stars in the wavelength region 4000–5400 Å with the spectrum of the comparison star HD 5223. Some of the prominent features seen in the spectra are marked on the figure.

$(J - H)$ and $(J - K)$. By considering the uncertainties arising from different sources such as uncertainties in the Strömgren photometry, reddening and the calibration of the absolute flux in the infrared, Alonso et al. (1996) estimated an uncertainty of ∼90 K in $T_{\rm eff}$ determination. The broad-band $(B - V)$ colour is often used for the determination of $T_{\rm eff}$; however, the $(B - V)$ colour of a giant star depends not only on $T_{\rm eff}$ but also on the metallicity of the star and the molecular carbon absorption features, because of the effect of CH molecular absorption in the B band. For this reason, we have not used the empirical $T_{\rm eff}$ scale for the $(B - V)$ colour indices. Since there is a negligible difference between the 2MASS infrared photometric system and the photometry data measured on the TCS system used by Alonso et al. (1998) in deriving the $T_{\rm eff}$ scales, we have used the empirical $T_{\rm eff}$ scales with 2MASS photometric data. We have further assumed that the effects of reddening on the measured colours are negligible. In estimating $T_{\rm eff}$ from the $T_{\rm eff}$ versus $(J - H)$ and $T_{\rm eff}$ versus $(V - K)$ relations, we had to adopt a value for the metallicity of the stars, as the metallicity of these stars is not known. We assumed the metallicity of the stars to be the same as that of their closest comparison star. This assumption has definitely affected the accuracy of the $T_{\rm eff}$ measurements. Estimated effective temperatures are listed in Table 3.

For a reliable determination of metallicity, effective temperatures and chemical compositions of these stars, observation at high resolution is necessary. High-resolution spectra will also enable us to make an accurate measurement of $^{12}C/^{13}C$ ratios.

6.2 Isotopic ratio $^{12}C/^{13}C$ from molecular band depths

The carbon isotopic ratio $^{12}C/^{13}C$ provides an important probe of stellar evolution but the low resolution of the spectra does not allow a meaningful estimation of this ratio.

We have estimated the ratio of the molecular band depths using the bands of (1,0) $^{12}C^{12}C$ λ4737 and (1,0) $^{12}C^{13}C$ λ4744. For a majority of the sample stars, from the depths of the molecular bands we find the ratio $^{12}C/^{13}C \sim 3$, with the exception of three stars for which this ratio is 7, 13 and 77, respectively. The ratios are presented in Table 3. This ratio measured on the spectra of the well-known CH stars HD 26, 5223 and 209621 are respectively 5.9, 6.1 and 8.8. Tsuji et al. (1991) suggested two kinds of CH stars: one with very high $^{12}C/^{13}C$ ratio and the other with values less than about 10. Our estimated ratios of $^{12}C/^{13}C$ are consistent with this.

Several explanations of the significance of the range of values of $^{12}C/^{13}C$ ratios have been put forward in terms of the stars' evolutionary scenarios. One explanation for a lower value of the $^{12}C/^{13}C$ ratio is that, generally, the $^{12}C/^{13}C$ ratio and total carbon abundances decrease due to convection, which dredges up the products of the internal CNO cycle to the stellar atmosphere in the ascending red giant branch (RGB). If it reaches the asymptotic giant branch (AGB) stage, fresh ^{12}C may be supplied from the internal He-burning layer to the stellar surface, leading to an increase of $^{12}C/^{13}C$ ratio again. Since the abundance anomalies observed in CH giants are believed to have been originated by the transfer of mass from a now extinct

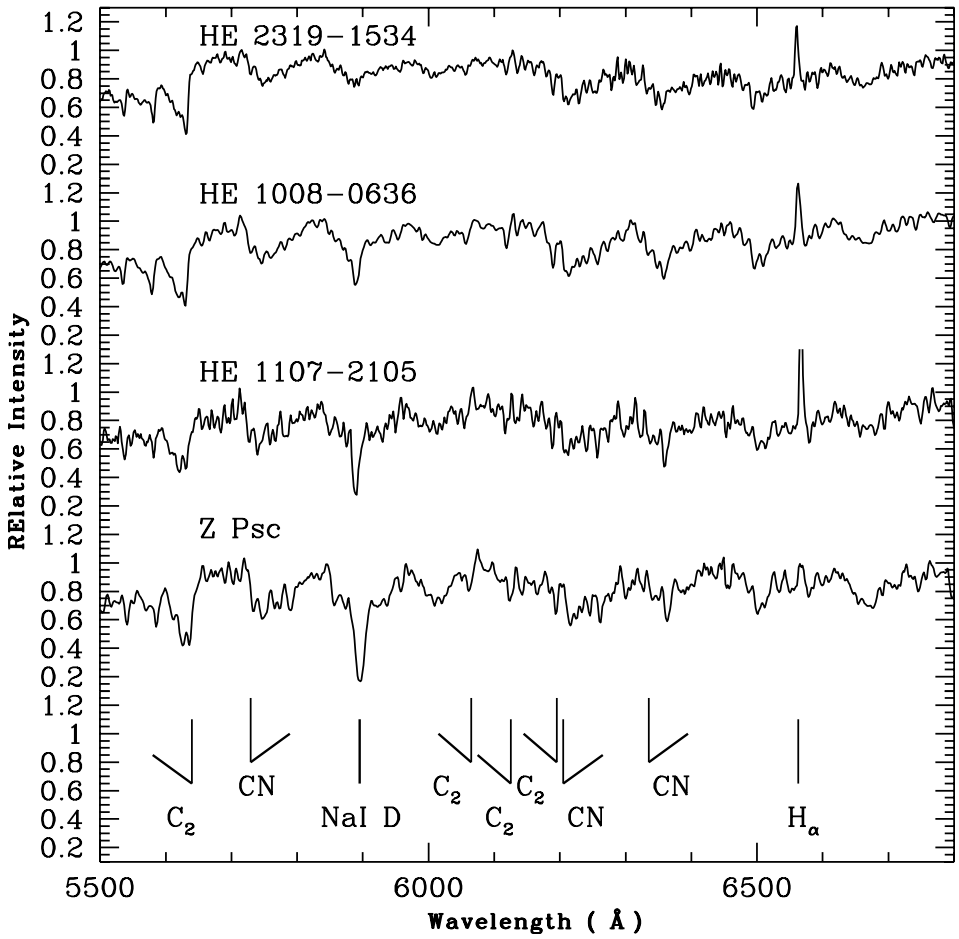

Figure 8. A comparison of the spectra of the candidate C-N stars HE 2319−1534, 1008−0636 and 1107−2105 with the spectrum of Z Psc in the wavelength region 5500–6800 Å. The bandheads of the prominent molecular bands, Na I D and Hα are marked on the figure. Hα is seen strongly in emission in the spectra of the HE stars.

AGB companion, the CH giant's atmosphere should be enhanced in triple-α products from the AGB star's interior – primarily ^{12}C. This explanation favours stars that give high $^{12}C/^{13}C$ ratios. Low carbon isotopic ratios imply that the material transferred from the now unseen companion has been mixed into the CN-burning region of the CH star or constitutes a minor fraction of the envelope mass of the CH star, thus giving isotopic ratios typical of stars on their first ascent of the giant branch.

7 CONCLUDING REMARKS

Large samples of high-latitude carbon stars such as that reported by Christlieb et al. (2001) allow a search for different kinds of carbon stars; the present work is a step in this direction. The sample of carbon star candidates offered by Christlieb et al. being high-latitude objects, with smaller initial masses and possibly lower metallicity, it is likely that a reasonable fraction of them could be CH stars. Identification of several CH stars and a description of their spectra are the main results of this paper. Another effort is known to be under way (Marsteller et al. 2003; Beers et al. 2003) to carry out a medium-resolution spectroscopic study of the complete sample of stars from Christlieb et al. (2001). From the sample list we have acquired spectra for 91 stars in the first phase of observation. Out of these, 51 objects were found to exhibit strong C_2 molecular bands in their spectra, of which 13 stars have low flux below about 4300 Å; 25 objects show weak or moderate CH and CN bands; 12 objects show weak but detectable CH bands in their spectra; and three objects do not show any molecular bands due to C_2, CN or CH. As an example, in Fig. 9 we show three spectra: a spectrum of HE 0443−1847, which exhibits very weak molecular bands due to CN around 4215 Å and a weak *G* band of CH around 4300 Å (but no C_2 molecular bands); a spectrum of HE 0930−0018, which shows a weak signature of the *G* band of CH around 4300 Å; and a spectrum of HE 1227−3103, which does not show any molecular bands due to C_2, CN or CH.

Although, spectroscopically, the appearance of strong C_2 molecular bands is an obvious indication of a star being a carbon star, the conventional definition of a carbon star is a star with C/O $\geqslant 1$ (Wallerstein & Knapp 1998). Hence if one adopts this conventional definition, the non-appearance of any C_2 molecular bands will not necessarily disqualify a star from being a carbon star, as this does not exclude the condition C/O $\geqslant 1$, which at our resolution of the spectra is not derivable.

Westerlund et al. (1995) defined dwarf carbon stars as having $(J-H) \leqslant 0.75(H-K) \geqslant 0.25$ mag. None of the stars occupies a region defined by these limits in the $(J-H)$ versus $(H-K)$ plane. With respect to $(J-H)$ and $(H-K)$ colours, there is a clear separation between the C-N type stars and dwarf carbon star populations: there are CH stars with $(J-H) \leqslant 0.75$ but their $(H-K)$ values are less than the lower limit of 0.25 mag set for dwarf carbon stars. We find that the sample of stars under investigation

Table 3. Estimated effective temperatures ($T_{\rm eff}$) of the candidate CH stars.

Star No.	$T_{\rm eff}$			$^{12}C/^{13}C$
	$(J-K)$	$(J-H)$	$(V-K)$	
HE 0017+0055	3919.1	4124.4	–	1.3
HE 0038−0024	3783.8	3929.2	4306.2	1.9
HE 0043−2433	4263.8	4271.3	4379.3	–
HE 0110−0406	4405.6	4444.0	–	2.1
HE 0111−1346	4449.5	4481.0	–	2.5
HE 0151−0341	4619.2	4696.5	4912.7	1.7
HE 0308−1612	4274.8	4369.2	–	2.8
HE 0314−0143	3454.4	3561.6	–	76.8
HE 0319−0215	4188.9	4314.8	4480.4	4.7
HE 0322−1504	4054.8	4293.7	4614.6	2.2
HE 0457−1805	4097.6	4513.4	4165.5	–
HE 0507−1653	4740.2	4846.3	4983.1	6.7
HE 0518−2322	4680.9	4689.1	–	–
HE 1027−2501	–	–	–	1.8
HE 1056−1855	4280.5	4427.3	–	–
HE 1145−0002	3665.5	3905.5	3691.2	1.4
HE 1125−1357	3708.6	3897.9	3910.2	3.7
HE 1204−0600	3910.0	4102.6	3881.6	1.7
HE 1211−0435	4710.3	4476.0	4732.4	3.7
HE 1304−2046	4073.0	4200.9	4061.1	1.7
HE 1305+0132	3931.4	4061.2	4131.2	1.4
HE 1425−2052	4038.5	4179.1	3824.0	1.7
HE 1418+0150	3781.1	4042.8	–	1.5
HE 1429−0551	4367.4	4800.0	–	1.9
HE 1446−0112	3891.9	4160.2	3854.9	1.8
HE 1523−1155	4524.2	4491.1	4380.8	2.5
HE 1524−0210	3826.9	3942.1	4611.2	2.3
HE 1528−0409	4666.7	4662.4	4388.4	2.4
HE 2144−1832	3922.2	4226.4	–	2.1
HE 2145−1715	4019.1	3862.1	4214.1	2.2
HE 2207−0930	3628.5	3751.7	3736.5	1.4
HE 2207−1746	4378.8	4448.4	–	3.2
HE 2218+0127	5544.6	5631.3	–	4.2
HE 2221−0453	4231.7	4487.1	4163.8	12.6
HE 2339−0837	4592.6	4499.1	5104.5	2.3
HD 26				5.9
HD 209621				8.8
HD 5223				6.1

comprises mostly CH stars and a small number of C-N and C-R stars.

We have derived the effective temperatures of the candidate CH stars from correlations of Alonso et al. (1996) making use of $(J-K)$, $(J-H)$ and $(V-K)$ colour indices. They vary over a wide range of temperature with an average of ±240 K. These temperature estimates provide a preliminary temperature check for the programme stars and can be used as starting values in deriving atmospheric parameters from high-resolution spectra using model atmospheres. For the majority of the sample stars, we find a carbon isotopic ratio $^{12}C/^{13}C \sim 3$, with the exception of the three stars HE 0507−1653, 2221−0453 and 0314−0143, for which this ratio is 7, 13 and 77, respectively. It was suggested by Tsuji et al. (1991) that there could be two kinds of CH stars: one with very high $^{12}C/^{13}C$ ratio, and the other with values ∼10. Our $^{12}C/^{13}C$ estimates are consistent with this. This range of ratios is the same as found for the Population II giants and globular cluster giant stars (Vanture 1992). Different evolutionary scenarios are held responsible for the two groups of CH stars, one with high and the other with low $^{12}C/^{13}C$ ratios.

From radial velocity survey, CH stars are known to be binaries. For the moderately metal-poor classical CH stars ([Fe/H] ∼ −1.5), a scenario for abundance anomalies and the origin of carbon was proposed in which the carbon-enhanced star is a member of a wide binary system that accreted material from a former primary, during the AGB phase of the latter, as described by McClure & Woodsworth (1990). In such a scenario, CH stars with large $^{12}C/^{13}C$ ratios indicate that their atmosphere is enhanced in triple-α products. The process of convection dredges up the products of the internal CNO cycle to the stellar atmospheres in the ascending RGB, and this leads to a decrease in or a small value of the $^{12}C/^{13}C$ ratio and a small total carbon abundance. On reaching the AGB stage, the $^{12}C/^{13}C$ ratio increases again due to the receipt of fresh ^{12}C supplied from the internal helium-burning layer to the stellar surface. According to the models of McClure (1983, 1984) and McClure & Woodsworth (1990), the CH binaries have orbital characteristics consistent with the presence of a white dwarf companion; these stars have conserved the products of a carbon-rich primary and survived until the present in the Galactic halo.

However, in the case of a few carbon-enhanced, metal-poor stars (subgiants), monitoring of radial velocity over a period of eight years did not reveal radial velocity variations greater than 0.4 km s^{-1}, which is counter to the mass transfer scenario for these stars (Norris et al. 1997a; Aoki et al. 2000; Preston & Sneden 2001). Furthermore, it is expected that the star we observe today should display an enrichment of s-process elements, produced by the former primary in its AGB phase, while the carbon-enhanced metal-poor star CS 22957−027 (Norris et al. 1997b; Bonifacio et al. 1998), as well as the stars reported by Aoki et al. (2000), do not exhibit this behaviour. The carbon-enhanced, metal-poor stars that do show s-process enrichment provide strong observational constraints for theoretical models of the structure, evolution and nucleosynthesis of early-epoch AGB stars, and permit studies of the s-process operating at very low metallicities. It was shown by Goriely & Siess (2001) that, even in the absence of iron seeds, efficient production of s-process elements can take place at zero metallicity provided protons are mixed into carbon-rich layers producing ^{13}C, which acts as a strong neutron source via the $^{13}C(\alpha,n)^{16}O$ reaction. The recent discovery of carbon-enhanced, metal-poor stars with strong overabundances of Pb support these predictions (Aoki et al. 2000; Van Eck et al. 2001). Thus CH stars, being the most prominent of the few types of heavy-element stars that exist in both the field of the Galaxy and globular clusters, are an important class of objects which can provide some of the very few direct observational tests to stellar evolution theory.

While the spectra of the stars listed in Table 1 are discussed in the present work, the analysis and description of the spectra of the stars listed in Table 2 will be discussed in a subsequent work.

ACKNOWLEDGMENTS

We thank the staff at IAO and at the remote control station at CREST, Hosakote, for assistance during the observations. This work made use of the Simbad astronomical data base, operated at CDS, Strasbourg, France, and the NASA ADS, USA. I am grateful to the referee, Professor Timothy Beers, for his many constructive suggestions, which have improved considerably the readability of the paper. The author would also like to thank Professor N. K. Rao for his guidance in the observational program, and helpful suggestions.

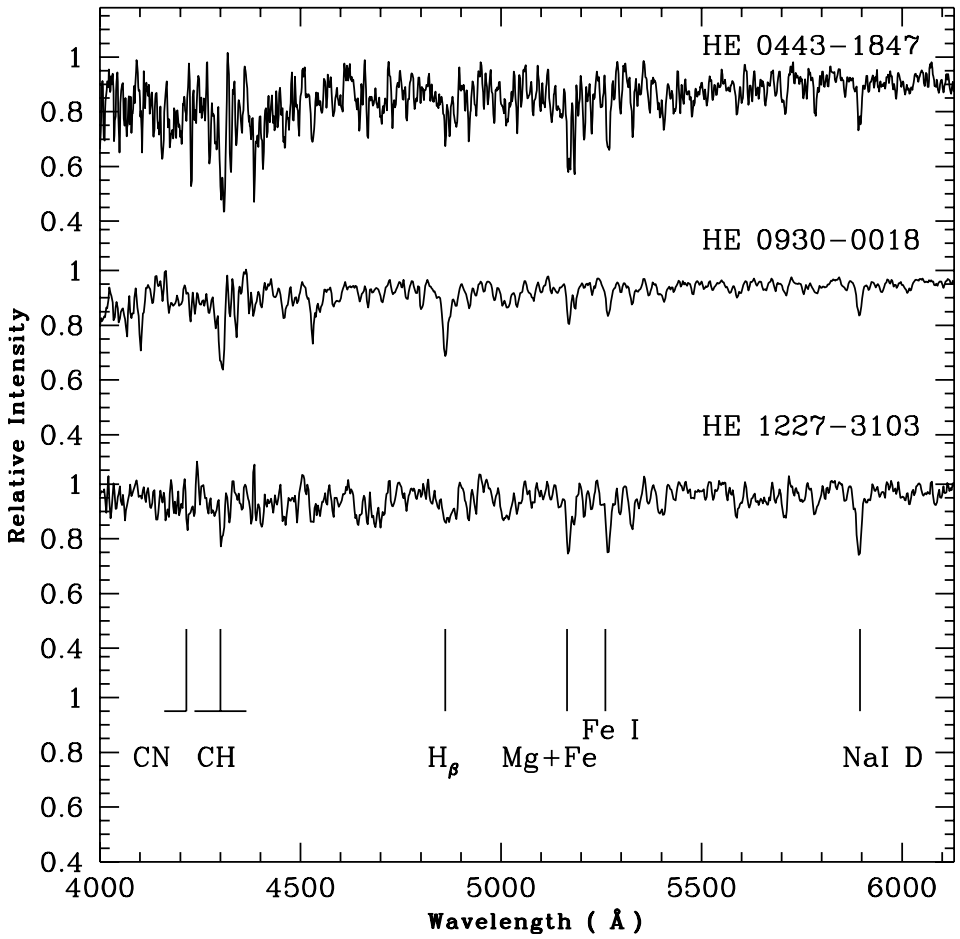

Figure 9. Three examples of the spectra of HE stars in the wavelength range 4000–6130 Å: HE 0443−1847, which exhibits very weak molecular bands due to CN around 4215 Å and a weak *G* band of CH around 4300 Å (but no C_2 molecular bands); HE 0930−0018, which shows a weak signature of the *G* band of CH around 4300 Å; and HE 1227−3103, which does not show the presence of any molecular bands due to C_2, CN or CH in its spectrum.

REFERENCES

Alonso A., Arribas S., Martinez-Roger C., 1996, A&A, 313, 873
Alonso A., Arribas S., Martinez-Roger C., 1998, A&AS, 131, 209
Aoki W., Tsuji T., 1997, A&A, 317, 845
Aoki W., Norris J. E., Ryan S. G., Beers T. C., Ando H., 2000, ApJ, 536, L97
Aoki W., Norris J. E., Ryan S. G., Beers T. C., Ando H., 2002, ApJ, 567, 1166
Barnbaum C., Stone R. P. S., Keenan P., 1996, ApJS, 105, 419
Beers T. C., 1999, in Gibson B. K., Axelrod T. S., Putman M. E., eds, ASP Conf. Ser. Vol. 165, The Third Stromlo Symposium: The Galactic Halo. Astron. Soc. Pac., San Francisco, p. 202
Beers T. C., Preston G. W., Shectman S. A., 1992, AJ, 103, 1987
Beers T. C., Lucatello S., Gratton R. G., Carretta E., Christlieb N., Cohen J. G., 2003, in 25th IAU Meeting, Joint Discussion 15, Elemental Abundances in Old Stars and Damped Lyman-Alpha Systems.
Bonifacio P., Molaro P., Beers T. C., Vladilo G., 1998, A&A, 332, 672
Christlieb N., Green P.J., Wisotzki L., Reimers D., 2001, A&A, 375, 366
Dominy J. F., 1984, ApJS, 55, 27
Goriely S., Siess L., 2001, A&A, 378, L25
Green P. J., Margon B., 1994, ApJ, 423, 723
Green P. J., Margon B., Anderson S. F., MacConnell D. J., 1992, ApJ, 400, 659
Green P. J., Margon B., Anderson S. F., Cook K. H., 1994, ApJ, 434, 319
Harding G. A., 1962, Observatory, 82, 205
Hartwick F. D. A., Cowley A. P., 1985, AJ, 90, 2244
Hill V., Francois P., Spite M., Primas F., Spite F., 2000, A&A, 364, L19
Hill V. et al., 2002, A&A, 387, 560
Lambert D. L., Gustafsson B., Eriksson K., Hinkle K. H., 1986, ApJS, 62, 373
McClure R. D., 1983, ApJ, 268, 264
McClure R. D., 1984, ApJ, 280, L31
McClure R. D., Woodsworth A. W., 1990, ApJ, 352, 709
Marsteller B. et al., 2003, AAS Meeting 203, #112.16
Norris J. E., Ryan S. G., Beers T. C., 1997a, ApJ, 488, 350
Norris J. E., Ryan S. G., Beers T. C., 1997b, ApJ, 489, L169
Norris J. E., Ryan S. G., Beers T. C., Aoki W., Ando H., 2002, ApJ, 569, L107
Preston G. W., Sneden C., 2001, AJ, 122, 1545
Rossi S., Beers T. C., Sneden C., 1999, in Gibson B. K., Axelrod T. S., Putman M. E., eds, ASP Conf. Ser. Vol. 165, The Third Stromlo Symposium: The Galactic Halo. Astron. Soc. Pac., San Francisco, p. 264
Totten E. J., Irwin M. J., 1998, MNRAS, 294, 1
Totten E. J., Irwin M. J., Whitelock P. A., 2000, MNRAS, 314, 630
Tsuji T., Tomioka K., Sato H., Iye M., Okada T., 1991, A&A, 252, L1
Van Eck S., Goriely S. I., Jorissen A., Plez B., 2001, Nat, 412, 793
Vanture A. D., 1992, AJ, 104, 1997
Wallerstein G., 1969, ApJ, 158, 607
Wallerstein G., Knapp G., 1998, ARA&A, 36, 369
Westerlund B. E., Azzopardi M., Breysacher J., Rebeirot E., 1995, A&A, 303, 107
Yamashita Y., 1975, PASJ, 27, 325
Zinn R., 1985, ApJ, 293, 424

This paper has been typeset from a TEX/LATEX file prepared by the author.